DOI: 10.17344/acsi.2017.4034 *Acta Chim. Slov.* **2018,** *65,* 354–364

Scientific paper

Capsicum annuum Fruit Extract: A Novel Reducing Agent for the Green Synthesis of ZnO Nanoparticles and Their Multifunctional Applications

Haraluru Shankraiah Lalithamba,[1,*] Mahadevaiah Raghavendra,[1] Kogali Uma,[1] Kalanakoppal Venkatesh Yatish,[1] Das Mousumi,[2] and Govindappa Nagendra[3]

[1] *Department of Chemistry, Siddaganga Institute of Technology, B.H. Road, Tumakuru - 572 103, Karnataka, India*

[2] *Department of Biotechnology, Siddaganga Institute of Technology, B.H. Road, Tumakuru - 572 103, Karnataka, India*

[3] *Fakultat fur Chemie und Chemische Biologie, Technische Universität Dortmund, Germany*

** Corresponding author: E-mail: lalithambasit@yahoo.co.in*

Received: 28-11-2017

Dedicated to the 111th Birthday (born April 1, 1907) of Dr. Sree Sree Sree Shivakumara Mahaswamiji, Siddaganga Matt, Tumakuru, Karnataka, India.

Abstract

A simple, efficient and convenient method for the preparation of zinc oxide (ZnO) nanoparticle was described. Several parameters like size and morphology of the prepared nanoparticles were characterized thorough a variety of analytical techniques such as XRD, FT-IR, UV-Vis, SEM, and EDX. The prepared ZnO nanoparticles were successfully used as catalyst for the formylation of amino acid esters and biodiesel synthesis. Further, the synthesized formamide esters were well characterized through HRMS, ^{1}H NMR and ^{13}C NMR analysis and subjected for the *in vitro* antibacterial and antifungal tests and the results indicated that some of them showed promising activity against targeted bacterial pathogens.

Keywords: Zinc oxide NPs; Solution combustion; Formylation; Biodiesel production; Biological activities

1. Introduction

Zinc oxide is a multifunctional material with its unique physical and chemical properties, such as high chemical stability, high electrochemical coupling co-efficient, high range of radiation absorption and high photostability.[1] ZnO as a catalyst with high specific surface area[2] finds the potential use in electronics, optoelectronics, laser technology and is made possible because of broad energy band (3.37a eV), high bond energy (60 MeV), thermal and mechanical stability at room temperature.[3] ZnO NPs have fascinated the research world through its significant applications in pigment electronics, spintronics and piezoelectricity fields.[4] Nano structured material ZnO has the ability to generate power, which also finds an extensive application in self-power generating devices for medical, wireless technologies and sensor applications.[5] ZnO shows diverse group of growth morphologies such as nano rings, nano springs, nano combs, nanowires and nano cages.[6] These have been synthesized using solid-vapour phase thermal sublimation technique[7] under specific growth condition. ZnO nanoparticles have drawn attention due to their antimicrobial activity; this finds application in food packaging.[8] Biocompatibility and biodegradability makes it a material of interest for biomedicine and in pro-ecological systems.[9] Nano ZnO plays a vital role as a semiconductor photo catalyst for UV-induced degradation of methylene blue[10] and doped ZnO also exhibits good optical and electrical properties.

Dhiman *et al.* reported the synthesis of Fe-doped ZnO nanoparticles by solution combustion method.[11] Recently, there are several attempts for the green biosynthesis approach for the preparation of ZnO, SnO_2, silver and reduced graphene oxide-silver (RGO-Ag) nanocomposites using leaf extracts of *Plectranthus amboinicus* and *Corymbia citriodora* as a reducing agent at different temperatures. The synthesized NPs showed a superior photocatalytic, catalytic activity towards dye molecules degradation and

also investigated the electrochemical properties of ZnO, RGO-Ag.[12–16] It has been widely studied that, ZnO is a highly efficient catalyst for a plethora of organic reactions, such as Friedel–Crafts acylation, Beckmann rearrangements, synthesis of cyclic ureas from diamines, *N*-alkylation of imidazoles and ring-opening of epoxides.[17] Nehal and others synthesized the ZnO nanoparticles and studied the effect of annealing temperature on its particle size.[18] The prepared ZnO NPs were reported to be employed in various functional group transformations. Among the transformations, protection of reactive amino groups is commonly required in organic synthesis using formyl group.[19] Formylation of amine is one of the important protocol in organic synthesis and medicinal chemistry. Various formylating reagents such as formic acid-DCC, formic acid-EDCI, KF-alumina, and ammonium formate were employed.[20–23] The obtained formamides are the main class of organic intermediates, which act as Lewis bases.[24] Synthesis of formamide was also achieved by the reaction of isocyanate and formic acid in the presence of DMAP,[25] acetic formic anhydride,[26] and metallic zinc.[27] Literature survey reveals that, many catalysts were used for the *N*-formylation of amines with formic acid, such as amberlite IR-120,[28] TiO_2-P25 or sulfated titania,[29] and HEU zeolite.[30] *N*-formylation of amines using hydroxylamine hydrochloride as a catalyst under neat condition was reported by Deepali agarwal and co-workers.[31] Using amine and formic acid in the presence of a catalytic amount of thiamine hydrochloride, formamide derivatives have been synthesized in excellent yields.[32] Nano MgO, ZnO, and CeO_2 were also used as catalysts in the synthesis of formamides.[33–35] Chandra shekhar *et al.* reported the facile *N*-formylation of amines using Lewis acids such as, $FeCl_3$, $AlCl_3$, and $NiCl_2$ as novel catalysts.[36] There are various methods to prepare nano structured particles. Some of the methods include chemical vapour deposition,[37] hydrothermal,[38] precipitation,[39] and sol-gel method.[40] The conventional physical and chemical methods available for the synthesis of NPs have adverse effects like critical temperature conditions and pressure, expensive chemicals, toxic byproducts *etc.*

Herein, green synthesis of zinc oxide nanoparticles using eco-friendly and non-toxic *Capsicum annuum* extract was reported. Capsaicin is an alkaloid found mainly in the fruit of the Capsicum genus, which provides spicy flavour andhas pharmacological effects to determine specific applications, such as for weight-loss and as an analgesic.[41] Literature survey confirms that the capsaicin has anti-bacterial and anti-diabetic properties.[42] *Capsicum annuum* is a rich source of ascorbic acid generally known as vitamin C, a very essential antioxidant for human nutrition.[43] This method has several benefits such as simple procedure, inexpensive reagents and good stability of nanoparticles. The solid catalyst is of great importance because of its advantages such as non-hazardous nature, requirement in small proportions and easier reaction workup.

Biodiesel is recognized as an alternative fuel due to its similar bearing with diesel fuel. Existing days, research has been intensive to the alternative sources of energy.[44,45] Commonly, biodiesel is a mixture of fatty acid methyl ester (FAME), which is synthesized from vegetable oil, waste oils and animal fat through transesterification reaction. Homogeneous catalysts such as KOH, NaOH, CH_3OK, and CH_3ONa show a favorable catalytic efficiency with various drawbacks such as generation of waste water, corrosion of equipment.[46] In display, solid heterogeneous catalysts are favorable for biodiesel synthesis because of environmentally friendly, easy separation, and could be reused many times.[47] Many solid acid catalysts like zeolite,[48] WO_3/ZnO_2,[49] and sulphated zirconia[50] were suitable for esterification reaction under 60–75 °C. In fact, solid acid catalysts (phosphotungstic acid, 12-tungstophosphoric acid, and ionic liquids) are used for the esterification and transesterification through one pot method. Meanwhile, solid base catalysts such as $Ca(OCH_3)_2$,[51] CaO[52], and KOH/Al_2O_3 were used in transesterification reaction at mild condition. Among the transition metal oxides, zinc oxide was reported the best catalyst for transesterification due to its minimum weight loss and high activity in the reaction.[53] Currently, application of nano catalysts for biodiesel synthesis has drawn much attention, as a result of easy separation of products, less pollution, higher catalytic activity and reusability.[54] Recently, nano catalysts such as CaO,[55] $Ti(SO_4)O$,[56] $KF/CaO\text{-}Fe_3O_4$,[57] Ag/ZnO[58], and mixed oxide TiO_2-ZnO[59] were used for biodiesel production. Presently, non-edible oils are used for biodiesel production to reduce edible oil conflict among food and fuel purpose. In this study, *Buteamonosperma* oil (non-edible) is used for biodiesel production and this plant belongs to a fabaceae family which is native to Indian subcontinent and seeds contain 23% of oil.[60,61]

In the present work, we report the synthesis of ZnO NPs through solution combustion by using *Capsicum annuum* extract as the combustible fuel and the obtained ZnO is employed as catalyst for the *N*-formylation of amino acid esters and biodiesel production. Further, the synthesized formamide derivatives were subjected for biological activities.

2. Experimental Section

2. 1. General

All chemicals were purchased from Sigma-aldrich and Merck and used without purification. The pathogenic bacterial strains were procured from National chemical laboratory Pune, India. The *Capsicum annuum* fruits were collected from local market, Tumakuru district, Karnataka, India. TLC analysis was carried out using pre-coated silica gel F_{254}. The phase identity and crystalline size of ZnO NPs were characterized through shimadzu powder X-ray diffractometer (PXRD-7000). IR spectra were re-

corded on Bruker Alpha-T FT-IR spectrometer (KBr windows, 2 cm^{-1} resolution), SEM analysis on Hitachi-7000 Scanning Electron Microscopy and elemental analysis was obtained from energy dispersive X-ray diffraction (EDX). UV–Vis diffused reflectance spectra were analyzed through Lambda-35 (Parkin Elmer) spectrophotometer. Mass spectra were recorded on a Micromass Q-ToF Micro Mass Spectrometer. Melting points were taken on open capillaries, ^{1}H NMR, and ^{13}C NMR spectra of the formamide derivatives were done on a Bruker AMX 400 MHz spectrometer using Me_4Si (tetramethylsilane) as an internal standard and $CDCl_3$ (deuterated chloroform) as a solvent.

2. 2. Synthesis of Nano Zinc Oxide Particles Through Solution Combustion Method

The *Capsicum annuum* fruit was collected and washed with distilled water. The whole mass was grinded to get the powder and then mixed with distilled water and boiled at 80 °C. After cooling to room temperature, the mixture was filtered using a Whatman filter paper no. 1 to obtain chilli extract. Zinc nitrate as precursor and *Capsicum annuum* fruit extract as fuel in the ratio of 4:1 were used for the synthesis of ZnO NPs through solution combustion method.[62] The solution was heated to 450 °C for 30 min and then dried in hot air oven for 4–5 h to obtain ZnO NPs in good yield.

2. 3. General Procedure for the Synthesis of Formamide Esters Using ZnO NPs

The prepared amino acid ester (1.0 mmol) was dissolved in dry DCM (dichloromethane) and neutralized with NMM (*N*-methyl morpholine) (1.5 mmol). To this solution, formic acid (2.0 mmol) was added at room temperature, followed by the addition of nano ZnO (0.5 mmol). The reaction mixture was stirred for 2 to 3 hours. The product was extracted into DCM and the organic layer was washed with hydrochloric acid solution (10 mL), sodium carbonate solution (15mL), water (15 mL) and brine (15 mL). It was dried over anhydrous sodium sulphate and concentrated under reduced pressure.

2. 4. Synthesis of Biodiesel Using ZnO NPs as a Catalyst

Transesterification reaction was carried out in a three necked round bottom flask equipped with reflux condenser on the middle neck, thermometer on the side neck and placed on the plate of the magnetic stirrer. In the beginning, 100 ml of *B. monosperma* oil was pre heated at 70 °C then a mixture of 2% wt. ZnO and 9:1 molar ratio of methanol to oil was added. The entire reaction was carried out at 65 °C for duration of 2 h. After the completion of reaction, the mixture was allowable to phase separation, the biodiesel (top layer), glycerine (middle layer) and catalyst (bottom layer) phase were separated. Then, the catalyst and glycerine were drained out and unreacted methanol was recovered from biodiesel. The obtained biodiesel was filtered to remove any dissolved zinc oxide catalyst.

3. Results and Discussion

3. 1. Characterization of ZnO NPs

XRD spectrum (Figure 1) has prominent peaks corresponding to the diffraction peaks at 2θ = 31°, 34°, 36°, 47°, 56°, 62° and 67° were indexed with the diffraction planes (100), (002), (101), (102), (110), (103) and (112) approve with JCPDS card no. 36–1451,[63] which confirms the hexagonal wurtzite structure of ZnO NPs. Average particle size (D) of synthesized NPs were found to be 33.26 nm using Scherer's formula. From the XRD spectrum, it is concluded that ZnO NPs synthesised by biologically initiated green synthesis conferred uniform size distribution fluctuates between 30 to 40 nm.

The average crystallite size of prepared sample was calculated by Debye-Scherrer's[64] formula i.e.

$$D = \frac{0.89\,\lambda}{\beta \cos\theta} \quad (1)$$

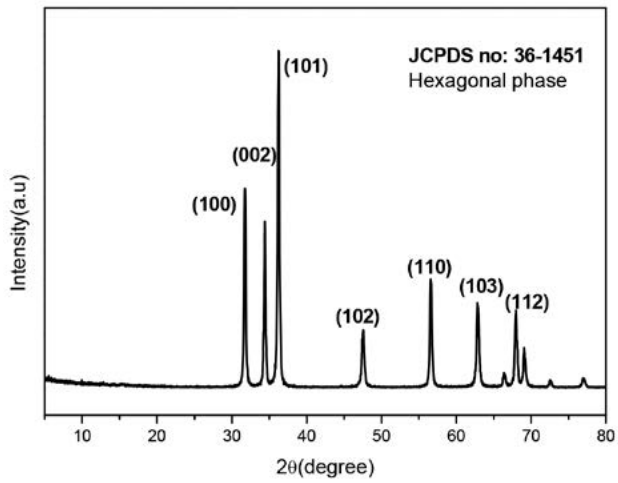

Figure 1. XRD pattern of ZnO NPs.

where, *D* is crystalline size, λ is X-ray wavelength (0.154 nm), β is full-width at half-maximum and θ is Bragg's angle. The average crystallite size of the ZnO NP was found to be 33.26 nm.

Figure 2(a) and 2(b) show DRS spectra and band gap plot of ZnO nanoparticles respectively. DRS spectrum reveals that the absorption is at ~ 400 nm. The Kubelka – Munk function[65,66] was utilized to determine the band gap energy (E_g) of ZnO NPs. The intercepts of the tangents to the plots of $[F(R_\infty)\ h\nu]^{1/2}$ versus photon energy (hν) were

shown in Figure 2(a) and 2(b). The Kubelka- Munk function F (R_∞) and photon energy (hν) can be calculated by following Equations (2), (3) and (4):

$$F(R_\infty) = \frac{(1-R_\infty)^2}{2R_\infty} \quad (2)$$

$$R_\infty = 10^{-A} \quad (3)$$

$$h\nu = \frac{1240}{\lambda} \quad (4)$$

where R_∞; reflection coefficient of the sample, A; the absorbance intensity of ZnO nanoparticles and λ; the absorption wavelength. The energy band gap value was found to 3.10 eV.

Figure 3 shows the SEM images of as prepared zinc oxide nano particles. Figure 3c is the enlarged part of 3b and 3a, which clearly shows that the particles are agglomerated cluster to form spongy cave like structures. The sizes of the particles are found to be in the 500 nm to 1 micrometer.

The Energy Dispersive X-ray Diffractive study was carried out for the prepared ZnO NPs to know about the elemental composition. The EDX spectrum confirms the

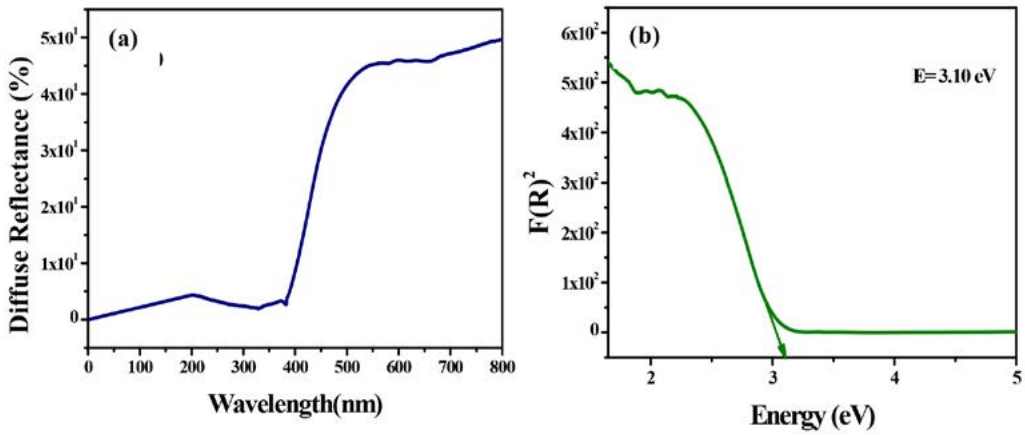

Figure 2. Diffuse reflectance spectrum (a) and direct band gap energy of ZnO (b).

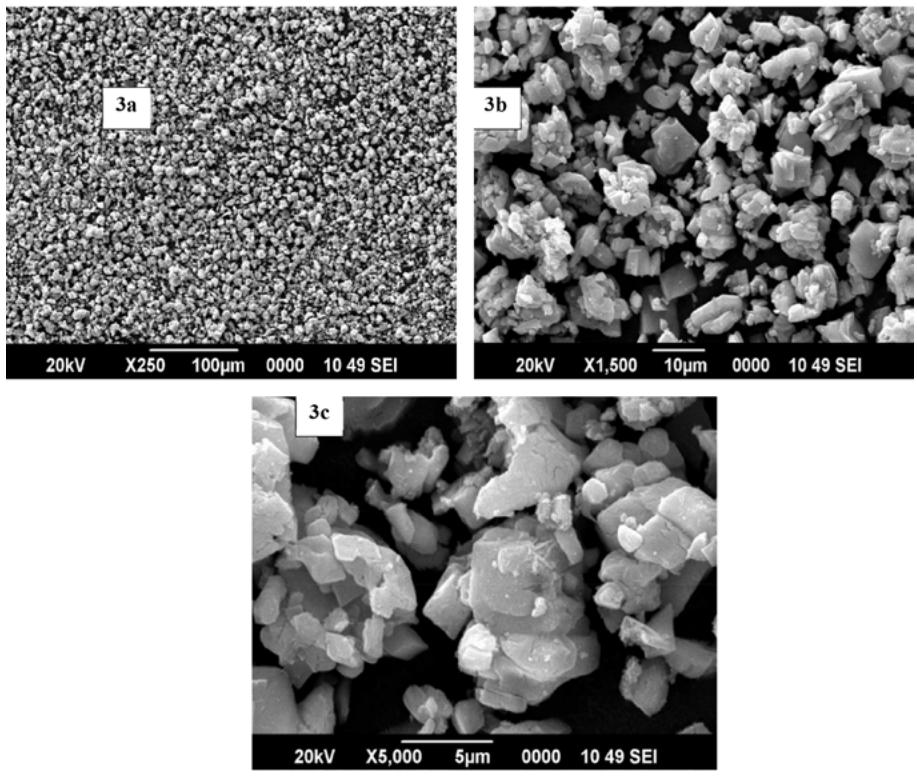

Figure 3. SEM image of ZnO nanoparticles.

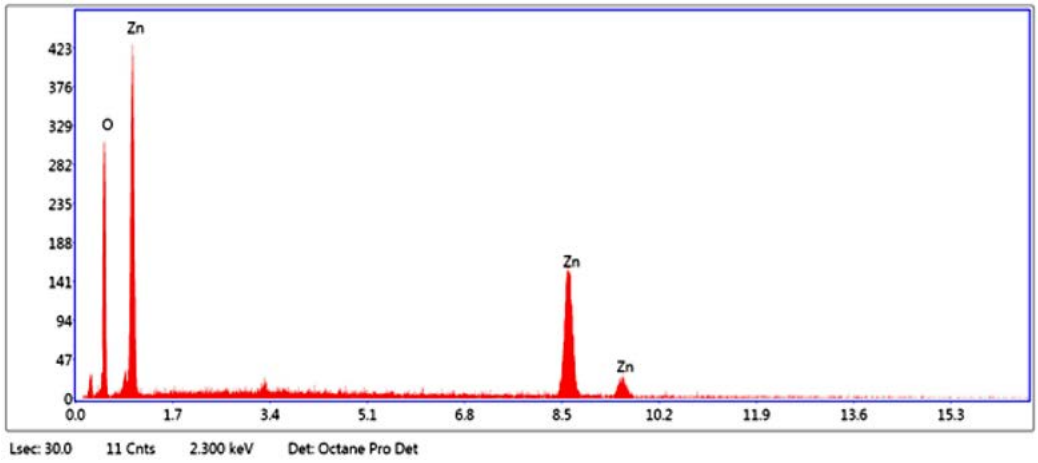

Figure 4. EDX spectrum of ZnO nanoparticles.

presence of zinc and oxygen signals and elemental analysis of the nanoparticle yielded 55.33% of zinc and 44.67% of oxygen.

Figure 5 is the FT-IR spectrum of ZnO NPs and the band in the region of 680–400 cm^{-1} is the characteristic peak of ZnO NPs. Thus, the formation of pure ZnO NPs at 535 cm^{-1} is evidenced by FT-IR[67] and the peak at 1122 cm^{-1} in FTIR spectrum is due to C-O stretching mode.[68] The peaks observed at 1628 cm^{-1} and 3500 cm^{-1} were due to the presence of -OH stretching and bending vibrations respectively assigned to the H_2O adsorption on the surface of metal.[69]

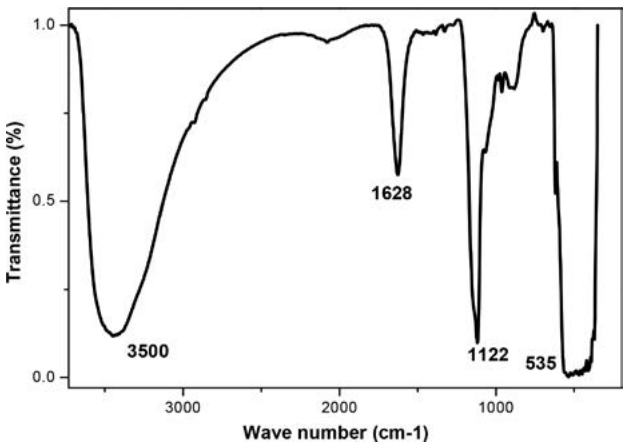

Figure 5. FTIR spectrum of ZnO nanoparticles.

Figure 6(a), (b) show the photoluminescence (PL) spectra of ZnO NPs recorded at room temperature. The recombination of photo generated free charge carriers leads to photoluminescence emission in semiconductor materials. The spectrum was recorded under UV excitation (375 nm) using Xenon lamp as source. The result obtained reveals that nano ZnO shows the strong emission peak at 600 nm (Figure 6(a)). The emission spectrum was monitored at 375 nm showed a broad emission at 600 nm was shown in

Figure 6(b). The broad 600 nm peak was due to the transition between single charged oxygen vacancies. The correlated color temperature was one of the essential parameter to know the color appearance of the light emitted by a light source with respect to a reference light source

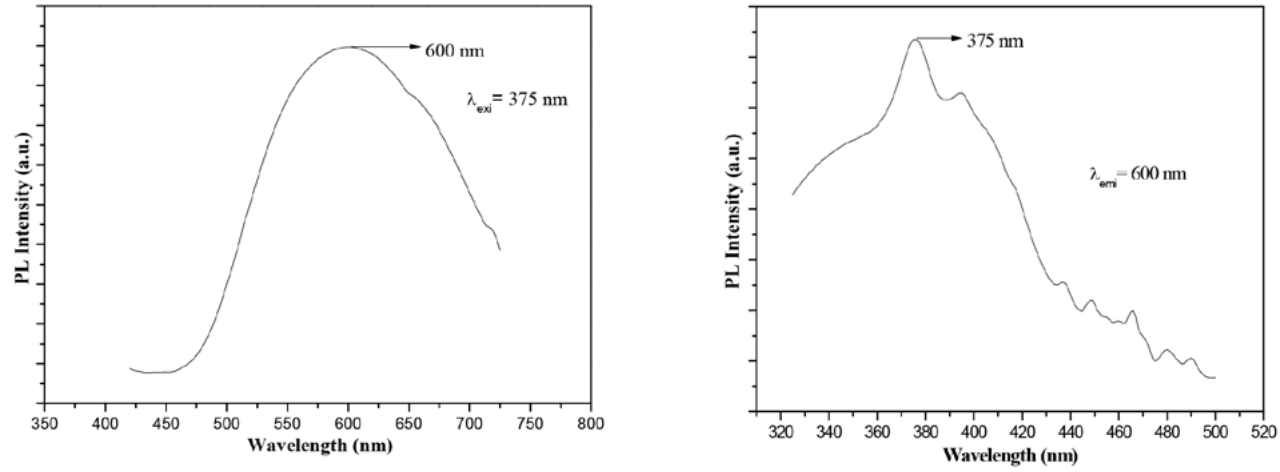

Figure 6. PL emission spectrum (a) and excitation spectrum (b) of nano ZnO.

when heated up to a specific temperature. The color clarity of any luminescent material was expressed in terms of chromaticity coordinates, called Commission International De I'Eclairage (CIE).

3. 2. Application of ZnO NPs as a Catalyst for the Formylation of Amino Acid Esters

In the current years, the use of metaloxides as a catalysts and reaction media has received considerable tremendous interest because of their high level of environmental compatibility, chemo selectivity and availability at low cost. Therefore, we explored the application of nano ZnO powder as an inorganic catalyst to carry out *N*-formylation of amino acid ester (1 mmol) in DCM with aq. 98% formic acid (1.5 mmol) at room temperature. Formamide derivative of amino acid ester was obtained in trace amount in the absence of ZnO catalyst, while good results were obtained with use of 0.5 mmol ZnO catalyst after same reaction conditions as mentioned. But less than 0.5 mmol considerably decreased the percentage of formamide esters and may took longer time for the completion of reaction. Using more than 0.5 mmol of ZnO has less effect on the final yield of the products. Thus, we found that 0.5 mmol of ZnO could efficiently catalyze the reaction for preparation of the desired products and observed that the excellent yield obtained using 1.5 mmol of formic acid. In literature survey Suresh babu *et al.* achieved successful synthesis of formamide derivatives of protected amino acids by the reaction of isocyanate with aqueous formic acid using DMAP as an organo catalyst.[70] However, this procedure suffers from the difficulties such as expensive reagents, highly toxic and may also require special care. Hence, it is necessary of convenient reagent for the synthesis of stable formamides in terms of economic viability and operational simplicity. Therefore, it is necessary to study this reaction using nano ZnO with a variety of amino acid esters as starting materials which were subjected to formylation reaction and the results were presented in Table 1. For the synthesis of titled compounds (**2a–h**), amino acid ester containing different aryl/alkyl groups prepared from thionyl chloride was dissolved in dry DCM and neutralized with NMM, to which aqueous formic acid was added followed by the addition of nano ZnO. The reaction mixture was stirred till the completion of the reaction (as monitored by TLC). After the simple work-up, desired products were obtained in good yield (Scheme 1). Using this procedure several formamide esters were synthesized from amino acid esters and characterized by their ^{1}H NMR, ^{13}C NMR and mass spectral studies.

Table 1. List of formamide esters prepared using ZnO NPs

Entry	Product	Yield (%)	M.p./ ºC
1	**2a**	90	162
2	**2b**	80	*Gum*
3	**2c**	89	188
4	**2d**	85	132
5	**2e**	79	*Gum*
6	**2f**	84	*Gum*
7	**2g**	85	158
8	**2h**	88	*Gum*

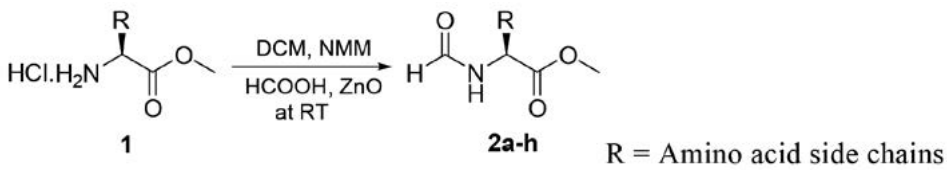

Scheme 1. Synthesis of *N*-formamide esters

3. 3. Spectral Data of the Synthesized Compounds:

N-formyl Ala-OMe (**2a**): % Yield 90, Solid, Melting Point: 162 ºC. ^{1}H NMR (400 MHz, $CDCl_3$) δ 1.39 (d, *J* = 8 Hz, 3H), 2.02 (s, 1H), 3.46 (s, 3H), 4.55 (m, 1H), 8.20 (s, 1H). ^{13}C NMR (100 MHz, $CDCl_3$) δ 17.5, 46.36, 52.0, 162.3, 170.1. MS: Cald. for $C_5H_9NO_3$ *m/z*: 131.06, found: 131.0576.

N-formyl Ser-OMe (**2b**): % Yield 80, Gum. ^{1}H NMR (400 MHz, $CDCl_3$) δ 1.81 (s, *2*H), 3.60 (s, 3H), 4.06 (m, 2H), 4.42 (m, 1H), 8.22 (s, 1H). ^{13}C NMR (100 MHz, $CDCl_3$) δ 51.4, 52.9, 60.5, 160.8, 171.0. MS: Cald. for $C_5H_9NO_4$ *m/z*: 147.05, found: 147.002.

N-formyl Tyr-OMe (**2c**): % Yield 89, Solid, Melting Point: 188 ºC. ^{1}H NMR (400 MHz, $CDCl_3$) δ 1.88 (s, 1H), 3.04 (m, 2H), 3.45 (s, 3H), 4.78 (m, 1H), 5.06 (s, 1H), 6.68 (d, *J* = 8 Hz, 2H), 6.80 (d, *J* = 8 Hz, 2H), 7.92 (s, 1H). ^{13}C NMR (100 MHz, $CDCl_3$) δ 36.4, 50.8, 51.6, 114.8, 129.3, 131.4, 155.0, 162.6, 171.5. MS: Cald. for $C_{11}H_{13}NO_4$ *m/z*: 223.08, found: 223.0802.

N-formyl Leu-OMe (**2d**): % Yield 85, Solid, Melting Point: 132 ºC.^{1}H NMR (400 MHz, $CDCl_3$) δ 1.06 (d, *J* = 8 Hz, 6H), 1.74–1.80 (m, 3H), 2.0 (s, 1H), 3.47 (s, 3H), 4.46 (m, 1H), 8.10 (s, 1H). ^{13}C NMR (100 MHz, $CDCl_3$) δ 22.4, 22.75, 40.34, 48.2, 51.62, 162.4, 170.8. MS: Cald. for $C_8H_{15}NO_3$ *m/z*: 173.11, found: 173.0998.

N-formyl Pro-OMe (**2e**): % Yield 79, Gum. ^{1}H NMR (400 MHz, $CDCl_3$) δ 1.60 (m, 2H), 1.68 (m, 2H), 2.65 (m, 2H),

3.53 (t, 1H), 3.62 (s, 3H), 8.0 (s, 1H).^{13}C NMR (100 MHz, $CDCl_3$) δ 22.8, 28.4, 43.92, 50.73, 58.02, 162.1, 172.0. MS: Cald. for $C_7H_{11}NO_3$ *m/z*: 157.07, found: 157.0711.

N-formyl Val-OMe **(2f)**: % Yield 84, Gum. ^{1}H NMR (400 MHz, $CDCl_3$) δ 1.08 (d, *J* = 8 Hz, 6H), 2.0 (s, 1H), 2.98 (m, 1H), 3.66 (s, 3H), 4.38 (d, *J* = 8 Hz, 1H), 8.0 (s, 1H). ^{13}C NMR (100 MHz, $CDCl_3$) δ 17.8, 29.92, 51.0, 54.7, 163.4, 171.2. MS: Cald. for $C_7H_{13}NO_3$ *m/z*: 159.09, found: 159.0898.

N-formyl Phe-OMe **(2g)**: % Yield 85, Melting Point: 158 ºC. ^{1}H NMR (400 MHz, $CDCl_3$)δ 2.0 (s, 1H), 3.02 (m, 2H), 3.48 (s, 3H), 4.75 (t, 1H), 7.08–7.20 (m,5H), 8.17 (s, 1H). ^{13}C NMR (100 MHz, $CDCl_3$) δ 37.6, 50.82, 51.7, 126.2, 127.5, 128.0, 138.65, 162.88, 171.1. MS: Cald. for $C_{11}H_{13}NO_3$ *m/z*: 207.09, found: 207.0930.

N-formyl Met-OMe **(2h)**: % Yield 88, Gum. ^{1}H NMR (400 MHz, $CDCl_3$) δ 1.86 (s, 1H), 2.04 (s, 3H), 2.20 (m, 2H), 2.38 (t, 2H), 3.55 (s, 3H), 4.40 (t, 1H), 8.11 (s, 1H). ^{13}C NMR (100 MHz, $CDCl_3$) δ 16.9, 29.64, 31.5, 50.12, 52.3, 163.82, 172.0. MS: Cald. for $C_7H_{13}NO_3S$ *m/z*: 191.06, found: 191.0602.

3. 4. Antibacterial and Antifungal Activity of Formamide Derivatives

The synthesized compounds were evaluated for their antibacterial activity against *E. coli* (MTCC 443) and *S. Aureus* (MTCC 5823). Lack of activity of the tested substances against Gram +ve bacteria could be explained by the differences in the structure of cell walls of Gram +ve and Gram -ve microorganisms. In most Gram +ve bacteria, the cell wall consists of many layers of peptidoglycan, forming a thick, rigid structure. Whereas, the cell walls of Gram –ve bacteria consist of one or a very few layers of peptidoglycan and a lipid-rich outer membrane.[71] Similar type of results employing different type of compounds such as Schiff's bases and amine derived from alkyl 2-(2-formyl-4-nitrophenoxy) alkanoates was recorded by Goszczyn´ska.[72] A contrasting difference in antibacterial activity employing Gram +ve and Gram –ve strains representing better susceptibility by *E. coli* than *S. aureus* employing novel benzothienopyrimidines compounds was shown.

In this study, the antibacterial screening indicated quite varied results among the tested samples as depicted in Table 2, 3, and 4 exhibiting antibacterial and antifungal activities respectively. For *E. coli* (MTCC 443), formamide ester derivatives of Ala, Tyr, Phe have shown good susceptibility over a wide volume range taken for a fixed concentration of samples (Table 2). Serine derivative has shown best result in comparison

to others at higher volume of fixed concentration of the sample tested. Rest of the samples were found to be resistant against the bacterial strain. A different result has been observed in terms of susceptibility pattern tested against *S. aureus* (MTCC 5823). Derivatives of Ala, Ser,

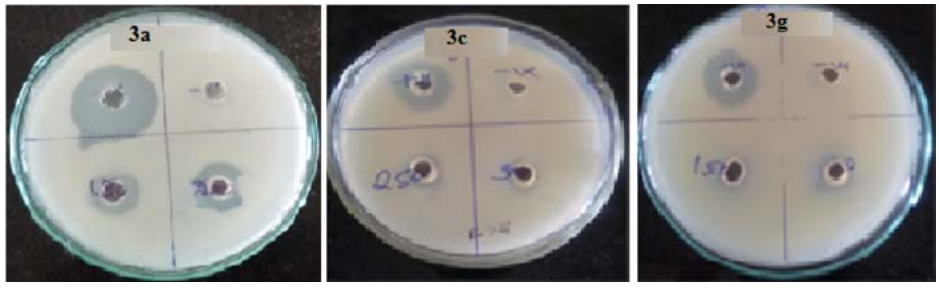

Figure 7. Photographs showing antibacterial activity of the formamides (3a, 3c and 3g) in agar well diffusion method with Gram -ve *Escherichia coli* bacteria.

Table 2. Antibacterial activity of standard and samples employing *E. coli*

Entry	Sample name *Escherichia coli*	Standard (Gentamicin)	*Sample concentration* (µl) 50	100	150	200	250	300
			Zone of Inhibition (mm)					
3a	OHCHN-Ala-OMe	++++	–	–	+	+	+	+
3b	OHCHN-Ser-OMe	++++	–	–	–	+	+	++
3c	OHCHN-Tyr-OMe	++++	–	–	–	+	+	+
3d	OHCHN-Leu-OMe	++++	–	–	–	–	–	–
3e	OHCHN-Pro-OMe	++++	–	–	–	–	–	+
3f	OHCHN-Val-OMe	++++	–	–	–	–	–	–
3g	OHCHN-Phe-OMe	++++	–	–	+	+	+	+
3h	OHCHN-Met-OMe	++++	–	–	–	–	–	–

Table 3. Antibacterial activity of standard and samples employing *S. Aureus*

Entry	Sample name *S. Aureus*	Standard (Gentamicin)	*Sample concentration* (µl) 50	100	150	200	250	300
			Zone of Inhibition (mm)					
3a	OHCHN-Ala-OMe	++++	–	–	–	–	–	–
3b	OHCHN-Ser-OMe	++++	–	–	–	–	–	–
3c	OHCHN-Tyr-OMe	++++	–	–	–	–	+	+
3d	OHCHN-Leu-OMe	++++	–	–	–	–	–	+
3e	OHCHN-Pro-OMe	++++	–	–	–	–	–	–
3f	OHCHN-Val-OMe	++++	–	–	–	–	–	+
3g	OHCHN-Phe-OMe	++++	–	–	–	–	–	+
3h	OHCHN-Met-OMe	++++	–	–	–	–	–	–

Zone of Inhibition: (–) 0–3mm; (+) 4–6 mm, (++) 7–9 mm, (+++) 10–12 mm, (++++) 12 mm

Table 4. Antifungal activity of standard and samples employing *Humicolafuscoatra*

Entry	Sample name *Humicolafuscoatra*	Standard (Fluconazole)	*Sample concentration* (µl) 50	100	150	200	250	300
			Zone of Inhibition (mm)					
3a	OHCHN-Ala-OMe	+++	+	–	–	+	+	–
3b	OHCHN-Ser-OMe	+++	–	+	+	+	+	+
3c	OHCHN-Tyr-OMe	+++	–	–	–	–	–	+
3d	OHCHN-Leu-OMe	+++	–	+	+	+	–	+
3e	OHCHN-Pro-OMe	+++	–	+	–	+	+	+
3f	OHCHN-Val-OMe	+++	–	+	+	+	+	–
3g	OHCHN-Phe-OMe	+++	–	+	+	+	+	+
3h	OHCHN-Met-OMe	+++	–	+	+	+	+	+

Zone of Inhibition: (–) 0–1 mm; (+) 2–4 mm, (++) 5–7 mm, (+++) 8 mm

Pro and Met were found to be resistant at fixed concentration with different range of volume from 50 to 300 µl. While, Tyr, Leu, Val and Phe derivatives have shown (Table 3) moderate susceptibility in comparison to Gram –ve *E. coli* (MTCC 443). All comparisons were done keeping in record the values of standard tested. Zones of inhibition (in mm) were measured at varying dilutions and depicted in the photographs of the culture plates of the best cases (Figure 7).

Summarization of antifungal activity has shown in Table 4. Derivatives of Ala, Tyr, Leu, Pro and Val have shown some activity in comparison to standard. While the derivatives of Phe, Ser, and Met have also shown good activity over a wide range of volume of samples (50–300 µl) tested for a fixed concentration. We are also measured the equivalent zones of inhibition (in mm) at varying dilutions and depicted in the photographs of the culture plates for the best cases (Figure 8).

The antimicrobial activity of formamide esters were evaluated against standard MTCC strains of Gram +ve and Gram -ve bacteria (standard strains: *Staphylococcus aureus* MTCC 5823, *Eschsrichia coli* MTCC 443) and a strain of fungi *Humicolafuscoatra* (MTCC 3938) by agar well diffusion method.[73] The optimum turbidity (<1.0) suitable for bacterial inoculum preparation was followed according to McFarland's test[74] employing Luria Bertani Broth for *E. coli* and Nutrient Broth for *S. aureus*. For fungal inoculum preparation 72 h incubation period was optimized for

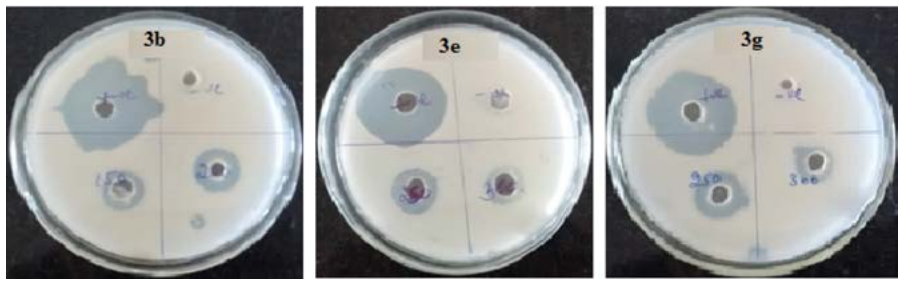

Figure 8. Photographs showing antifungal activity of the formamides (3b, 3e and 3g) in agar well diffusion method with *Humicolafuscoatra* bacteria.

choosing the culture suspension employing Potato dextrose broth pertaining to antifungal activity. The standards used were fluconazole at the conc. of 0.10 mg/ml and gentamicin of 0.003 mg/ml concentration (Plating volume 50 µl) for antifungal and antibacterial activity respectively. The wells of 6 mm diameter were punched employing a sterile cork borer into the Mueller hinton agar (MHA) having the test microorganisms at concentration about 5×10^6 CFU/ml for bacterial strains and 3×10^5 CFU/ml for fungi. The wells were filled with different volumes in a range from 50 µl to 300 µl, at the concentration of 0.10 mg/ml employing DMSO. The plates were incubated for 18 h and 36 h at 35 ± 1 °C for *E. coli* and *S. aureus* respectively. For antifungal activity employing the same method with potato dextrose agar plates were incubated for 72 h at 28 ± 1 °C. Antimicrobial activity was evaluated by measuring the inhibition zone against the test microorganisms using an antibiogram scale and standard measurement protocol was followed according to CLSI guidelines.[75,76]

3. 4. Application of ZnO NPs as a Catalyst for the Biodiesel Production

After transesterification of *Buteamonosperma* oil, the yield of biodiesel was found to be 82.7%. In order to evaluate the quality of biodiesel, the fuel properties of the biodiesel were determined according to ASTM D6751 standards as shown in the Table 5. The fuel properties such as kinematic viscosity (4.3 cSt), flash point (151 °C), acid value (0.2 mg KOH/g), calorific value (37790 kJ/kg), density (880 kg/m^3) and copper strip corrosion (1a) were within the range of ASTM standard. Schematic diagram of ZnO NPs catalyzed transesterification for the production of biodiesel is shown in the Figure 9.

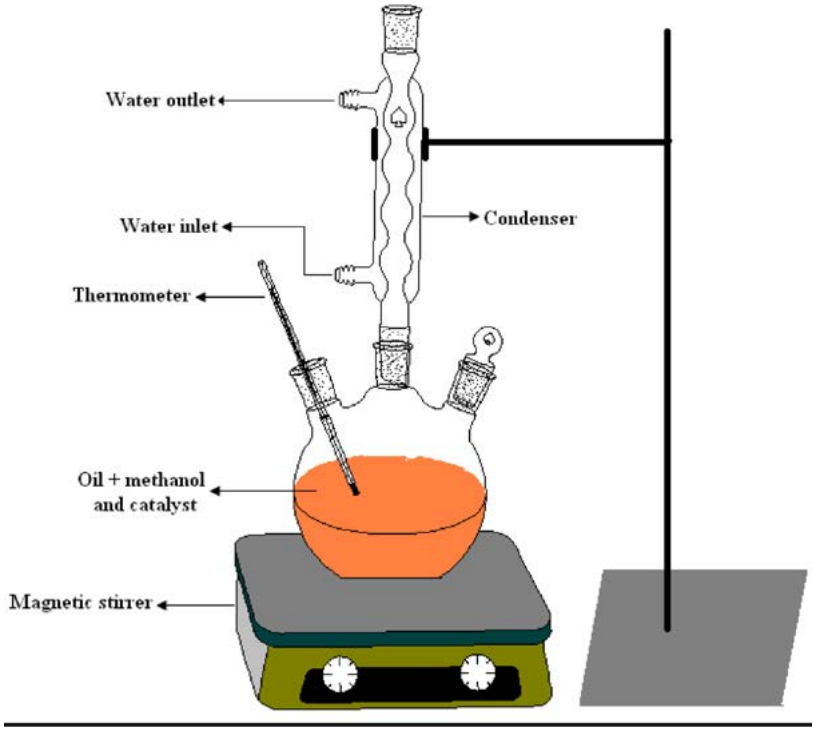

Figure 9. Schematic diagram of transesterification reaction.

Table 5. Fuel properties of *Buteamonosperma* biodiesel

Properties	Units	Testing procedure ASTM	BMME/ biodiesel	Biodiesel standard ASTM D6751
Viscosity at 40 °C	cSt	D445	4.3	1.9–6.0
Flash point	°C	D4052	151	>130
Acid value	mg KOH/g	D664	0.2	0.8 max
Calorific value	kJ/kg	D240	37790	–
Density	kg/m^3	D93	880	870–900
Copper strip corrosion, 50 °C, 3h	–	D130	1a	no. 3 max

BMME = Buteamonosperma methyl ester

4. Conclusions

Multifunctional ZnO nanoparticle has been synthesized *via* a simple solution combustion method using *Capsicum annuum* extract as a new fuel. The prepared NPs were characterized by UV-Vis DRS, XRD, SEM, and EDX and also evaluated its photoluminescence property. The method is environmental friendly and overcome the demerits of conventional physical and chemical methods of synthesis. In the presence of nano ZnO catalyst excellent yield of formamide esters and biodiesel have been obtained. The synthesized formamide esters were successfully characterized by ^{1}H NMR, ^{13}C NMR, and mass spectroscopy analysis. Finally, the formamide esters were subject to biological activities against bacterial pathogens and few of the molecules exhibited considerable biological activities.

5. Acknowledgements

We thank the Principal and Director of Siddaganga Institute of Technology, Tumakuru, Karnataka, for the research facilities. One of the authors (HSL) is thankful to the Vision Group of Science and Technology, Department of Information Technology, Biotechnology and Science & Technology, Government of Karnataka for providing funds under CISEE programme (GRD No. 472) to carry out the present research work by means of a sponsored project.

6. References

1. H. G. Reza, P. Ferdos, P. Hossein, B. R. Mosavar, *Orientational J. Chem*. **2015**, *31*, 1219–1221.
2. S. M. Hosseini, S. Hashem, *J. Org. Chem.* 2006, *71*, 6652–6654. **DOI:**10.1021/jo060847z
3. K. R. Agnieszka, J. Teofil, *Materials.* **2014**, *7*, 2833–2881. **DOI:**10.3390/ma7042833
4. D. Gnanasangeetha, T. D. Sarala, *J. Chem. Biolog. Phy. Sci*. **2013**, *4*, 238–246.
5. D. Indrani, A. Nitin, *Nanomaterials and Nanotech*. **2013**, *3*, 1–16. **DOI:**10.5772/56188
6. Z. W. Lin, *J. Phys. Condens. Matt.* **2004**, *16*, 829–858. **DOI:**10.1088/0953-8984/16/45/025
7. L. Miao, S. Tanemura, Y. Ieda, M. Tanemura, Y. Hayashi, H. Y. Yang, S. P. Lau, B. K. Tay, Y. K. Cao, *Surface Sci.* **2007**, *601*, 2660–2663. **DOI:**10.1016/j.susc.2006.12.011
8. J. J. Velázquez, V. D. Rodríguez, A. C. Yanes, J. del Castillo, J. Méndez-Ramos, *Appl. Phys. A*. **2012**, *108*, 577–583. **DOI:**10.1007/s00339-012-6929-z
9. G. M. Krishna, R. Jagannadha, *J. Engg. Trends and Tech.* **2015**, *26*, 272–275. **DOI:**10.14445/22315381/IJETT-V26P247
10. A. I. Muhammad, A. S. Iqbal, A. K. M. Rahman, A. M. Mahbubul, S. M. I. Saiful, A. H. Mohammad, *International J. Chemical Reactor Engg.* **2011***, 9*, 1–20.
11. P. Dhiman, K. M. Batoo, R. K. Kotnala, M. Singh, *Micro & Nano Lett.* **2012**, *7*, 1333–1335. **DOI:**10.1049/mnl.2012.0862
12. L. Fu, Z. Fu, *Ceramics International*. **2015**, *41*, 2492–2496. **DOI:**10.1016/j.ceramint.2014.10.069
13. L. Fu, Y. Zheng, Q. Ren, A. Wang, B. Deng, *J. Ovonic Res*. **2015**, *11*, 21–26.
14. Y. Zheng, Z. Wang, F. Peng, L. Fu, *Revista Mexicana de Ingenier´ıa Qu´ımica*. **2017**, *16*, 41–45.
15. Y. Zheng, A. Wang, W. Cai, Z. Wang, F. Peng, Z. Liu, L. Fu, *Enzyme and Microbial Technology*, **2016**, *95*, 112–117. **DOI:**10.1016/j.enzmictec.2016.05.010
16. Y. Zheng, Z. Wang, F. Peng, L Fu, *Brazilian Journal of Pharmaceutical Sciences*, **2016**, *52*, 781–786. **DOI:**10.1590/s1984-82502016000400023
17. Z. Ilona, S. Jakub, M. C. Anna, S. Kamil, L. Janusz, S. Jacinto, *Chem. Science Rev. and Lett.* **2015**, *4*, 735–745.
18. A. S. Nehal, M. El-Kemary, M. I. Ebtisam, *Nanoscience and Nanotech.* **2015***, 5*, 82–88.
19. S. Mojmir, A. H. E. Adam, H. E. H. Robert, *Org. Lett.* **2011**, *13*, 3952–3955. **DOI:**10.1021/ol201475j
20. J. Waki, J. Meienhofer, *J. Org. Chem.* **1977**, *42*, 2019–2020. **DOI:**10.1021/jo00431a046
21. F. M. F. Chen, N. L. Benoiton, *Synthesis*. **1979**, 709–710. **DOI:**10.1055/s-1979-28805
22. M. Miharam, Y. Ishino, S. Minakata, M. Komatsu, *Synthesis*. **2003**, *15*, 2317–2320.
23. P. G. Reddy, G. D. K. Kumar, S. Baskaram, *Tetrahedron*. **2000**, *41*, 9149–9151. **DOI:**10.1016/S0040-4039(00)01636-1
24. H. S. Mona, *Green Chem.-Envi. Benign Appro.* **2012**, *6*, 103–120.
25. V. V. Sureshbabu, N. Narendra, *Int. J. Pept. Res. Ther.* **2008**, *14*, 201–207. **DOI:**10.1007/s10989-008-9127-2
26. A. Jafar, H. Malak, S. Mehdi, H. Akbar, *Arkivok*. **2009**, *xi*, 123–129.
27. K. Joong-Gon, J. Doo Ok, *Bull. Korean Chem. Soc.* **2010**, *31*, 2989–2991. **DOI:**10.5012/bkcs.2010.31.10.2989
28. R. Madhusudana, T. M. V. Bhojegowda, N. Aatika, A. P. Mohamed, *Chinese J. Cat.* **2010**, *31*, 518–520.
29. B. Krishnakumar, M. Swaminathan, *J. Mol. Catalysis A: Chem.* **2011**, *334*, 98–102. **DOI:**10.1016/j.molcata.2010.11.002
30. B. Siavash, M. A. Babak, S. Mohammad, Z. Fereshteh, *Bull. Korean Chem. Soc.* **2012**, *33*, 2251–2254. **DOI:**10.5012/bkcs.2012.33.7.2251
31. D. Agarwal, A. Agrwal, A. Bairagi, V. K. Kasana, *Res. J. Chemical Sci.* **2014**, *4*, 54–57.
32. L. Min, M. Lei, H. Lihong, *Tetrahedron Lett.* **2010**, *51*, 4186–4188. **DOI:**10.1016/j.tetlet.2010.06.005
33. M. M. B. Reddy, S. Ashoka, G. T. Chandrappa, M. A. Pasha, *Catal. Lett.* **2010**, *138*, 82–87. **DOI:**10.1007/s10562-010-0372-6
34. S. S. Mohammad, M. Mehdi, R. Akbar, *Lett. in Org. Chem.* **2014**, *11*, 49–54. 35. M. Raghavendra, K. V. Yatish, H. S. Lalithamba, *Eur. Phys. J. Plus*. **2017**, *132*, 1–12.
36. S. A. Chandra, K. A. Ravi, G. Sathaiah, P. V. Luke, S. Madabhushi, R. P. Shanthan, *Tetrahedron Lett.* **2009**, *50*, 7099–7101. **DOI:**10.1016/j.tetlet.2009.10.006

37. R. Namita, *International J. Adv. in Engg. & Tech.* **2015**, *7*, 1806–1881.
38. R. Donya, B. H. Mohd Zobir, T. Y. Yun Hin, *Chm. Central J.* 2013, ***7,*** 1–10. **DOI:**10.1186/1752-153X-7-1
39. H. R. Ghorbani, F. P. Mehr, H. Pazoki, B. M. Rahmani, *Oriental J. Chem*. **2015**, *31*, 1219–1221.
40. S. Jurablu, M. Farahmandjou, T. P. Firoozabadi, *J. Sci. Islamic Republic of Iran.* **2015**, *26,* 281–285.
41. R. E. Maria de Lourdes, G. G. M. Edith, V. T. Erika, Molecules. **2011**, *16*, 1253–1270. **DOI:**10.3390/molecules16021253
42. S. D. Joao, *Food and Nutrition Sci.* **2012**, *3*, 1354–1374. **DOI:**10.4236/fns.2012.310179
43. A. O. Benin, H. Ahissou, Gbaguidi, F. Sanoussi, A. Houngbeme, A. Dansi, A. Sanni, *Int. J. Curr. Microbiol. App. Sci.* **2015**, *4*, 394–403.
44. S. Veena, H. H. Bassim, C. S. Yogesh, *Energy conversion and man*. **2016**, *122*, 52–62.
45. Muhammadi, Shabina, M. Afzal, S. Hameed, *Green Chem. Let. and Rev.* **2015,** *8*, 56–77. **DOI:**10.1080/17518253.2015.1109715
46. Z. Quan, Z. Heng, C. Fei, L. Hu, P. Hu, X. Wei, H. De-Yu, Y. Song, *J. Industrial and Engg. Chem.* **2015**, *31*, 385–392. **DOI:**10.1016/j.jiec.2015.07.013
47. *E. M. Shahid, Y. Jamal, Renewable and Sustainable Energy Rev.* ***2011****, 15*, *4732–4745.* **DOI:***10.1016/j.rser.2011.07.079*
48. Y. M. Park, J. Y. Lee, S. H. Chung, I. S. Park, S. Y. Lee, D. K. Kim, J. S. Lee, K. Y. Lee, *Bioresource Tech*. **2010**, *101*, S59–S61. **DOI:**10.1016/j.biortech.2009.04.025
49. K. H. Chung, B. G. Park, *J. Ind. Eng. Chem.* **2009**, *15*, 388–392. **DOI:**10.1016/j.jiec.2008.11.012
50. X. R. Chen, Y. H. Ju, C. Y. Mou, *J. Phys. Chem.* C. 2007, *111*, 18731–18737. **DOI:**10.1021/jp0749221
51. X. Liu, X. Piao, Y. Wang, S. Zhu, H. He, *Fuel.* 2008, *87*, 1076–1082. **DOI:**10.1016/j.fuel.2007.05.059
52. X. Liu, H. He, Y. Wang, S. Zhu, X. Piao, *Fuel.* 2008, *87*, 216–221. **DOI:**10.1016/j.fuel.2007.04.013
53. S. J. Yoo, H. S. Lee, V. Bambang, J. D. Kim, Y. W. Lee, *Bior. Technol.* **2010**, *101***,** 8686–8989.
54. S. Hu, L. Wen, Y. Wang, X. Zhen, H. Han, *Bior. Tech.* **2012**, *123*, 413–418. **DOI:**10.1016/j.biortech.2012.05.143
55. P. R. Pandit, M. H. Fulekar, *J. Environ. Manage.* 2017, *198*, 319–329. **DOI:**10.1016/j.jenvman.2017.04.100
56. G. Jabbar, H. Ali, L. Xiaojun, H. A. Mukhtar, *Appl.catalysis A: general.* 2016, *527*, 81–95. **DOI:**10.1016/j.apcata.2016.08.031
57. H. Shengyang, G. Yanping, W. Yun, H. Heyou, *Appl. Energy.,* 2011, *88*, 2685–2690. **DOI:**10.1016/j.apenergy.2011.02.012
58. G. Nagaraju, Udayabhanu, S. A. Shivaraj, M. S. Prashanth, K. V. Yathish, C. Anupama, D. Rangappa, *Mat. Res. Bull.* 2017, *94*, 54–63. **DOI:**10.1016/j.materresbull.2017.05.043
59. M. Rajesh, P. Shakkthivel, *Bior. Tech.* **2013**, *150*, 55–59. **DOI:**10.1016/j.biortech.2013.09.087
60. A. U. Khan, *Environ. Monit. Assess.* **2010**, *170*, 171–184. **DOI:**10.1007/s10661-009-1224-y
61. F. Rana, M. Avijit, *Int. J. Rese. Pharm. Chemi.* **2012,** *2*, 1035–1039.
62. M. Raghavendra, H. S. Lalithamba, B. S. Sharath, H. Rajanaika, *Scientia Iranica C.* **2017**, *24*, 3002–3013.
63. U. S. Rao, G. Srinivas, T. P. Rao, *Procedia Materials Science.* **2015***, 10,* 90–96.
64. S. P. Vinay, N. Chandrasekhar, *IOSR J. App. Chem.* **2017,** *10,* 57–63.
65. L. Wan, J. F. Li, J. Y. Feng, W. Sun, Z. Q. Mao, *Mater. Sci. Eng. B. 2007*, *139*, 216–220. **DOI:**10.1016/j.mseb.2007.02.014
66. J. Zhang, J. Xi, Z. Ji, *J. Mater Chem.* **2012**, *22*, 17700–17708. **DOI:**10.1039/c2jm32391e
67. S. Yedurkar, C. Maurya, P. Mahanwa, *Open Journal of Synthesis Theory and Applications*. **2016,** *5,* 1–14. **DOI:**10.4236/ojsta.2016.51001
68. D. Panchavarnam, S. Menaka, A. Anitha, M. Arulmozhi, *Int. J. ChemTech Research*. **2016**, *9*, 308–315.
69. S. N. Rao, M. V. B. Rao, American Journal of Materials Science. **2015,** *5*, 66–68.
70. N. S. Sudarshan, N. Narendra, H. P. Hemantha, V. V. Sureshbabu, *J. Org. Chem.* **2007**, *72*, 9804–9807. **DOI:**10.1021/jo701371k
71. J. B. Terry, *J. bacteriology.* 1999, *181*, 4725–4733.
72. G. Agata, K. Halina, F. Karol, *Med. Chem. Res*. 2015, *24*, 3561–3577. **DOI:**10.1007/s00044-015-1397-6
73. K. Uma, H. S. Lalithamba, M. Raghavendra, V. Chandramohan, C. Anupama, *Arkivoc*. **2016**, *4*, 339–351.
74. W. Irith, H. Kai, E. W. H. Robert, *Nature Proto.* 2008, *3*, 163–175. **DOI:**10.1038/nprot.2007.521
75**.** L. B. Reller, M. Weinstein, J. H. Jorgensen, M. J. Ferraro, *Clin Infect Dis.* **2009,** *49*, 1749–1755. **DOI:**10.1086/647952
76. S. P. Vinay, N. Chandrasekhar, *App. Nanoscience*. **2017**, *7*, 851–861. **DOI:**10.1007/s13204-017-0624-5

Povzetek

S preprosto, učinkovito in priročna metodo smo pripravili nanodelce cinkovega oksida ZnO. Različne parametre, kot so velikost in morfologija, tako pripravljenih nanodecev, smo preučevali z naslednjimi metodami: rentgenska praškovna difrakcija (XRD), infrardeča spektroskopija (FT-IR), UV-Vis spektroskopija, vrstično elektronsko mikroskopijo (SEM), in *energijsko* disperzijsko spektroskopijo rentgenskih žarkov (EDX). Nanodelce ZnO smo uporabili kot katalizatorje pri pripravi estrov aminokislin in v postopku sinteze biodizla. Tako sintetizirane estre smo karakterizirali z masno spektroskopijo (HRMS) in NMR spektroskopijo in z njimi opravili nekaj *in vitro* antibakterijskih in protiglivičnih testov. Nekateri izmed njih so pokazali obetajočo aktivnost proti bakterijskim patogenom.